



Examining axial diffusion of nitric oxide in the lungs using heliox and breath hold

Hye-Won Shin, Peter Condorelli and Steven C. George

Journal of Applied Physiology 100:623-630, 2006. First published Oct 6, 2005;
doi:10.1152/jappphysiol.00008.2005

You might find this additional information useful...

This article cites 32 articles, 24 of which you can access free at:

<http://jap.physiology.org/cgi/content/full/100/2/623#BIBL>

Updated information and services including high-resolution figures, can be found at:

<http://jap.physiology.org/cgi/content/full/100/2/623>

Additional material and information about *Journal of Applied Physiology* can be found at:

<http://www.the-aps.org/publications/jappl>

This information is current as of March 1, 2006 .

Journal of Applied Physiology publishes original papers that deal with diverse areas of research in applied physiology, especially those papers emphasizing adaptive and integrative mechanisms. It is published 12 times a year (monthly) by the American Physiological Society, 9650 Rockville Pike, Bethesda MD 20814-3991. Copyright © 2005 by the American Physiological Society. ISSN: 8750-7587, ESSN: 1522-1601. Visit our website at <http://www.the-aps.org/>.

Examining axial diffusion of nitric oxide in the lungs using heliox and breath hold

Hye-Won Shin,¹ Peter Condorelli,¹ and Steven C. George^{1,2}

Departments of ¹Biomedical Engineering and ²Chemical Engineering and Materials Science, University of California, Irvine, Irvine, California

Submitted 4 January 2005; accepted in final form 1 October 2005

Shin, Hye-Won, Peter Condorelli, and Steven C. George. Examining axial diffusion of nitric oxide in the lungs using heliox and breath hold. *J Appl Physiol* 100: 623–630, 2006. First published October 6, 2005; doi:10.1152/jappphysiol.00008.2005.—Exhaled nitric oxide (NO) is highly dependent on exhalation flow; thus exchange dynamics of NO have been described by multicompartment models and a series of flow-independent parameters that describe airway and alveolar exchange. Because the flow-independent NO airway parameters characterize features of the airway tissue (e.g., wall concentration), they should also be independent of the physical properties of the insufflating gas. We measured the total mass of NO exhaled ($A_{I,II}$) from the airways after five different breath-hold times (5–30 s) in healthy adults (21–38 yr, $n = 9$) using air and heliox as the insufflating gas, and then modeled $A_{I,II}$ as a function of breath-hold time to determine airway NO exchange parameters. Increasing breath-hold time results in an increase in $A_{I,II}$ for both air and heliox, but $A_{I,II}$ is reduced by a mean (SD) of 31% (SD 6) ($P < 0.04$) in the presence of heliox, independent of breath-hold time. However, mean (SD) values (air, heliox) for the airway wall diffusing capacity [3.70 (SD 4.18), 3.56 $\text{pl}\cdot\text{s}^{-1}\cdot\text{ppb}^{-1}$ (SD 3.20)], the airway wall concentration [1,439 (SD 487), 1,503 ppb (SD 644>)], and the maximum airway wall flux [4,156 (SD 2,502), 4,412 pl/s (SD 2,906)] using a single-path trumpet-shaped airway model that considers axial diffusion were independent of the insufflating gas ($P > 0.55$). We conclude that a single-path trumpet model that considers axial diffusion captures the essential features of airway wall NO exchange and confirm earlier reports that the airway wall concentration in healthy adults exceeds 1 ppm and thus approaches physiological concentrations capable of modulating smooth muscle tone.

gas exchange; trumpet model

NITRIC OXIDE (NO) can be detected in the exhaled breath, and the concentration, $F_{E,NO}$, may reflect the inflammatory status of the lungs (1, 3, 9, 14, 16, 31). However, NO exchange dynamics in the lungs are not yet fully developed, owing primarily to the unique gas-exchange characteristics of NO that include both airway and alveolar contributions (18, 27, 28).

Several techniques have been developed to partition $F_{E,NO}$ into airway and alveolar contributions (6, 7, 10, 18, 27, 28, 30) to provide information on region-specific pathobiology (8, 11–13, 17, 24–27). These methods include both vital capacity maneuvers and tidal breathing and generally alter exhalation flow to sample different gas-phase residence times in the airways. By doing so, the alveolar and airway regions can be characterized by flow-independent parameters which include the steady-state alveolar concentration ($C_{A,NO}$), the airway wall diffusing capacity ($D_{aw,NO}$), and either the airway wall con-

centration ($C_{aw,NO}$) or the maximum airway wall flux ($J'_{aw,NO}$, equal to the product $D_{aw,NO}\cdot C_{aw,NO}$) (6, 7).

Early models of NO exchange neglected axial diffusion of NO in the gas phase, as well as the increasing cross-sectional area of the airway tree with increasing airway generation (i.e., trumpet shape). These simplifications generated errors in the estimation of $C_{aw,NO}$ and $J'_{aw,NO}$ (21–23, 32). In addition, the variance of $D_{aw,NO}$ was larger than other parameters, and the accuracy depends on the residence time of the air in the airway compartment (25). A unique challenge in determining $D_{aw,NO}$ is the need to sample very low (<50 ml/s) exhalation flows (29). These very low exhalation flows can be difficult to perform, especially for young subjects and people with compromised lung function. Accurate estimation of $D_{aw,NO}$ is particularly interesting because initial studies suggest that it is elevated in asthma but may be independent of steroid use (24, 27), unlike $F_{E,NO}$ and $C_{aw,NO}$.

Recently, we have developed a new technique that focuses on the determination of the airway wall NO parameters ($C_{aw,NO}$, $D_{aw,NO}$, and $J'_{aw,NO}$) (21). The technique uses a series of different breath-holding times that significantly improves the accuracy of determining $D_{aw,NO}$ and suggests that, indeed, the estimation of $D_{aw,NO}$ also depends on axial diffusion and airway geometry.

The goal of the present study is to alter the rate of axial molecular diffusion of NO in the gas phase of the airway tree by using heliox (80% helium, 20% oxygen) as the insufflating gas and then accurately estimate airway wall NO parameters using our recently described breath-holding technique. Because the airway NO parameters characterize features of the airway wall or tissue, such as airway wall surface area, tissue thickness, and net rate of tissue production (28), they should be independent of the physical properties of the insufflating gas. To investigate this premise, our model of NO exchange must capture the relevant physical properties of the insufflating gas (e.g., rate of molecular diffusion), including the space it occupies (e.g., airway geometry).

METHODS

Experiment

Subjects. Nine healthy adults (age 21–38 yr, five female) participated in the study (Table 1). All subjects had a ratio of forced expiratory volume in 1 s to forced vital capacity (FEV_1/FVC) of >0.75 at the time of testing. In addition, all subjects had no history of smoking at any time and no history of cardiovascular, pulmonary, or neurological diseases. The Institutional Review Board at the Uni-

Address for reprint requests and other correspondence: S. C. George, Dept. of Biomedical Engineering, 204 Rockwell Engineering Center, Univ. of California, Irvine, Irvine, California 92697-2715 (e-mail: scgeorge@uci.edu).

The costs of publication of this article were defrayed in part by the payment of page charges. The article must therefore be hereby marked “advertisement” in accordance with 18 U.S.C. Section 1734 solely to indicate this fact.

Table 1. Physical characteristics of subjects

Subject No.	Gender	Age, yr	Height, in.	Body Weight, lb	Iwgt, lb	Vaw, ml	*Vaw, ml	FVC		FEV ₁		FEV ₁ /FVC	
								Liters	% Predicted	Liters	% Predicted	%	% Predicted
1	M	38	69	145	160	198	182	5.16	104	4.04	100	78	96
2	F	36	59	104	100	136	124	3.50	121	2.96	118	85	98
3	F	34	59	94	100	134	117	3.31	114	2.81	110	85	97
4	F	28	64	112	120	148	124	3.50	91	3.01	98	86	108
5	M	24	71	214	172	196	198	5.61	102	4.18	88	75	87
6	F	23	64	120	120	143	134	3.81	106	3.51	112	92	106
7	M	23	70	205	166	189	206	5.84	110	5.19	114	89	104
8	F	21	62	120	110	131	125	3.54	103	3.2	105	90	101
9	M	25	66	144	148	173	208	5.88	123	4.41	109	75	89
Mean		28.0	64.9	140	133	161	157	4.46	108	3.70	106	83.9	98.3

Iwgt, ideal body weight based on gender and ethnicity; Vaw; airway volume defined by the cumulative volume of generations 0–17; *Vaw, airway volume defined by the subject age (yr) plus ideal body weight (lb) (29); FVC, forced vital capacity; FEV₁, forced expiratory volume in 1 s; M, male; F, female.

versity of California, Irvine approved the protocol, and written, informed consent was obtained from all subjects.

Protocol. The breath-hold technique has been previously described in detail (21). Briefly, each subject performed a series of breath-hold maneuvers (5-, 10-, 15-, 20-, and 30-s breath hold) using either air or heliox as the insufflating gas during inspiration from functional residual capacity to total lung capacity. We have previously demonstrated that a tidal breathing wash-in period of heliox for 2 min before the inspiration of heliox and the breath hold does not significantly impact exhaled NO concentration (22) and thus was not included in the present protocol. The presence of heliox increases the molecular diffusivity of NO in the gas phase from 0.23 to 0.52 cm²/s relative to air (19). Exhalation flow after a breath hold was not controlled but was generally >200 ml/s to ensure evacuation of the airway space in ~2 s. A positive pressure >5 cmH₂O was maintained during the breath hold and exhalation to prevent nasal contamination (2). A schematic of the experimental apparatus has been previously presented (29). After indexes of NO exchange dynamics were measured, general spirometry including FVC and FEV₁ were measured in all subjects (Vmax229; Sensormedics, Yorba Linda, CA) by using the best performance (Table 1) from three consecutive maneuvers.

Airstream analysis. A chemiluminescence NO analyzer (NOA280, Sievers, Boulder, CO) was used to measure the exhaled NO concentration. The instrument was calibrated on a daily basis using a certified NO gas (45 ppm NO in 100% N₂ for air calibration and 45 ppm NO in 100% He for heliox calibration, Sievers). The zero-point calibration was performed with an NO filter (Sievers) immediately before the collection of a profile. Calibration with ≥80% of carrier gas (either nitrogen or helium as in the case of air or heliox, respectively) balanced with oxygen resulted in a negligible change in the response of the instrument (<2% for helium). The flow rate and pressure signals were measured by using a pneumotachometer (RSS100HR, Hans Rudolph, Kansas City, MO). The pneumotachometer was calibrated before each subject and set to provide the flow in units of STPD and pressure in units of cmH₂O. The software of the pneumotachometer accounts for changes in gas properties (e.g., viscosity) when using heliox as the insufflating gas.

Empirical data analysis. Experimental exhalation profiles after breath hold from air and heliox breathing were characterized empirically (independent of a mathematical model or “model independent”) by the peak or maximum observed concentration in phase I and II (Fig. 2A) of the exhalation profile, C_{NO peak}; the width of phase I and II, W₅₀, defined as the exhaled volume in which the NO concentration was greater than 50% of C_{NO peak}; V_{I,II}, the total exhaled volume of phase I and II; and A_{I,II}, the total mass or volume of NO (area under the curve) in phase I and II.

Model Development and Simulation

Trumpet model. Mathematical models to estimate airway wall NO parameters were developed for two cases: 1) trumpet airway in the absence of axial diffusion (T), and 2) trumpet airway in the presence of axial diffusion (T-AD). Details of these models, including the derivation of the governing equations and solutions, have been previously presented (21), and only the salient features will be described. For each subject, airway geometry was characterized by appropriately scaling the lengths and diameters of Weibel’s data of the human airway tree (4, 33), on the basis of the conducting airway volume (Vaw) of generations 0–17 of each subject (4, 33). The trumpet shape of the airway (15, 20, 23) is shown in Fig. 1, and was captured using the following relationship between airway cross-sectional area (A_c) and axial position, z (21):

$$A_c = A_{c,1} \left(\frac{z}{z_1} \right)^{-m} \quad (1)$$

where the exponent $m = 2$ provides an excellent match to the data of Weibel (33). The remaining generations (generations 18–23), including the respiratory and terminal bronchioles and the alveoli, are lumped together and assumed to be at C_{ANO}. Because reported values of C_{ANO} are generally <2 parts per billion (ppb), much lower than those observed in the airway tree during the breath-hold times of the present technique, C_{ANO} was set to zero as one of the boundary conditions (21).

Parameter estimation using different breath-hold times. Utilizing five different breath-hold times, two model-dependent, airway wall NO exchange parameters (Daw_{NO} and Caw_{NO}) from the two different models (i.e., T and T-AD) were uniquely determined (21) for each subject by matching the total mass of NO (A_{I,II}) accumulated in the airway gas phase during breath hold as a function of breath-hold time. The model-predicted values of the area under the curve in phase I and II, A_{I,II}^{*}, are referenced to the experimental data, A_{I,II}, by minimizing the root mean square error between the model prediction and experimental data. On the basis of the governing equations of the model, A_{I,II}^{*} depends on the airway wall NO parameters Daw_{NO} and Caw_{NO} (21). Once Daw_{NO} and Caw_{NO} were determined, J_{aw,NO} was calculated as the product of Caw_{NO} and Daw_{NO}.

Statistics. Data were analyzed by one-way and two-way repeated-measures ANOVA, followed by paired or unpaired *t*-tests as appropriate, if the ANOVA analysis demonstrated statistical significance ($P < 0.05$). All variables were assumed to be normally distributed, and all statistical tests were performed on raw data scores. Outliers were defined by raw values that exceeded three standard deviations from the mean. A P value < 0.05 was considered statistically significant.

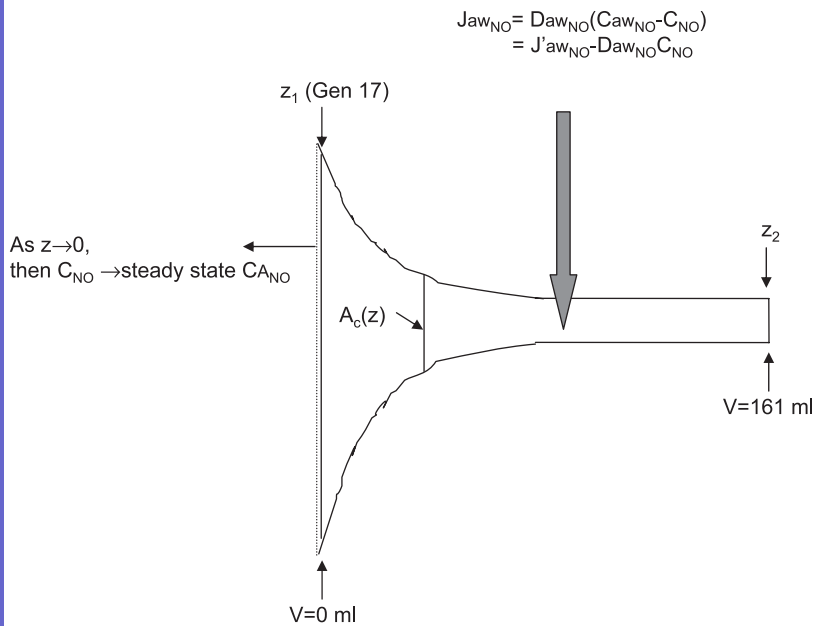


Fig. 1. Schematic of the trumpet-shaped human airway tree through 17 generations based on the symmetric bifurcating structure of Weibel (33). The cumulative cross-sectional area for any axial position, z , for the trumpet is calculated on the basis of the cumulative cross-sectional area of all of the airways at that position. As z approaches zero, exhaled nitric oxide (NO) concentration in the gas phase of the airways [C_{NO} , in parts per billion (ppb)] approaches the steady-state alveolar concentration (C_{awNO}). For simplicity, C_{awNO} is set to zero for the present simulations. D_{awNO} , airway wall diffusing capacity; C_{awNO} , airway wall concentration; J_{awNO} , airway wall flux; J'_{awNO} , maximum airway wall flux; V , volume; A_c , airway cross-sectional area.

RESULTS

Figure 2B presents a representative single tracing for the exhaled NO concentration profile as observed by the analytical instrument ($C_{NO\text{ obs}}$), exhalation flow, and pressure for inspiration of air using 20-s breath-hold time. Figure 2C presents the representative composite (average of all subjects) $C_{NO\text{ obs}}$ for air and heliox using a 20-s breath-hold time. The composite profile was attained by taking the mean exhaled concentration at equivalent exhaled volume intervals in the nine healthy subjects. A decrease in total mass of NO exhaled in phases I and II ($A_{I,II}$) was observed when heliox was used as the insufflating gas (36% reduction in heliox breathing), although $C_{NO\text{ peak}}$ was not statistically lower.

$C_{NO\text{ peak}}$, W_{50} , $V_{I,II}$, and $A_{I,II}$ for all nine subjects are presented in Fig. 3 to demonstrate model-independent differences in the exhaled NO profile as a function of breath-hold time as well as the differences between air and heliox breathing. For both air and heliox breathing, $C_{NO\text{ peak}}$ (Fig. 3A) and $A_{I,II}$ (Fig. 3D) were both strong positive functions of breath-hold times for all nine subjects. However, breath-hold time did not impact W_{50} or $V_{I,II}$ (Fig. 3, B and C). $C_{NO\text{ peak}}$ did not depend on the presence of heliox; however, W_{50} and $A_{I,II}$ (except 5-s breath hold) were all significantly reduced in the presence of heliox, independent of breath-hold times. $V_{I,II}$ tended to be lower in the presence of heliox but only reached statistical significance for breath-hold times of 15 and 20 s.

The determined airway wall NO parameters using a model which accounted for or neglected axial diffusion (T and T-AD) are presented in Fig. 4 for both air and heliox. Both models can accurately simulate the increase in $A_{I,II}$ with increasing breath-hold time. For air, the maximum deviation between $A_{I,II}^*$ and $A_{I,II}$ for any of the breath-hold times were 14.9 and 18.6% for T and T-AD, respectively. R^2 (coefficient of determination) values were 0.92 and 0.96 for T and T-AD, respectively. For heliox, the maximum deviation between $A_{I,II}^*$ and $A_{I,II}$ for any

of the breath-hold times were 10.9 and 11.2% for T and T-AD, respectively, and R^2 values were 0.92 and 0.97.

The impact of axial diffusion for the trumpet geometry (T-AD) was substantial. For air, C_{awNO} and J'_{awNO} were significantly ($P < 0.001$ for C_{awNO} and $P = 0.003$ for J'_{awNO}) increased by more than eightfold and threefold, respectively; D_{awNO} was ($P = 0.06$) decreased by $\sim 75\%$. For heliox, C_{awNO} and J'_{awNO} were also significantly ($P < 0.001$ for C_{awNO} and $P < 0.001$ for J'_{awNO}) increased by more than 22-fold and 4-fold, respectively; D_{awNO} was ($P = 0.005$) decreased by $\sim 80\%$. Of note is the observation that determined airway wall parameters are independent of the insufflating gas when axial diffusion is included in the model (i.e., T-AD).

NO concentration as a function of airway volumetric position is shown in Fig. 5 for the T-AD model for both air and heliox breathing when breath-hold time was set to 30 s. Recall, for both cases, that total mass of NO within the airway tree is not different because this is the experimental variable for which the determined model parameters are chosen to match. Because estimated NO parameters do not depend on the insufflating gas for model T-AD, the mean parameter set determined from air (1,439 ppb for C_{awNO} and $3.70\text{ pl}\cdot\text{s}^{-1}\cdot\text{ppb}^{-1}$ for D_{awNO}) was used to generate the NO profile within the airway tree. The presence of heliox reduces the concentration of NO along the airway tree during breath hold but does not impact $C_{NO\text{ peak}}$.

During exhalation, the NO concentration profile in the airway tree exits the mouth and enters the sampling system. C_{ENO} represents the NO concentration exiting the mouth, whereas $C_{NO\text{ obs}}(t)$ represents the observed NO concentration by the instrument. As previously reported (21), $C_{NO\text{ obs}}(t)$ predicted by the model determined airway wall NO parameters (mean for all nine subjects, shown in Fig. 6) for T-AD (solid circles, calculated on the basis of experimental NO tracing results described in the APPENDIX) agrees well with that observed experimentally (open circles) for both air (Fig. 6A) and heliox

breathing (Fig. 6B). Although the total mass of NO exhaled from the airway tree is not changed, the maximum $C_{NO\ obs}(t)$ (i.e., $C_{NO\ peak}$) is only 9–16% of the maximum $C_{E_{NO}}$ for air and only 3–6% for heliox breathing, depending on the breath-hold time.

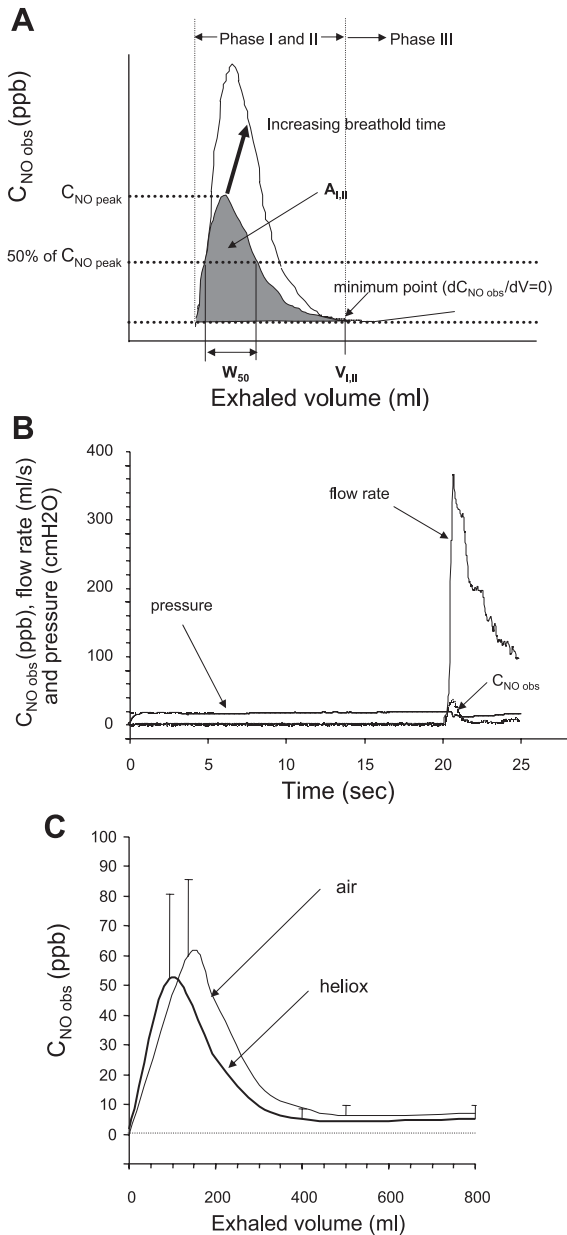


Fig. 2. A: model-independent parameters characteristic of the exhalation profile in phase I and II are defined schematically. $C_{NO\ obs}$, exhaled NO concentration observed experimentally from the analytical instrument; $C_{NO\ peak}$, maximum concentration of NO in phase I and II; W_{50} , width of the phase I and II peak calculated by taking the volume at which the exhaled concentration is larger than 50% of $C_{NO\ peak}$; $V_{I,II}$, volume of phase I and II; $A_{I,II}$, total mass of NO (area under the curve, which is shown as a shaded region) in phase I and II. The distinction between phase I and II and phase III is the point of zero slope (minimum point) in the exhalation profile as previously described (29). Upper curve is a schematic representation of the exhalation profile for a longer breath-hold time. B: representative experimental exhaled profile after 20-s breath hold to present NO, flow rate, and pressure tracing. C: composite or mean of the 9 healthy subjects, experimental NO exhalation profile (error bars are standard deviation) is presented for 20-s breath-hold maneuver for air and for heliox.

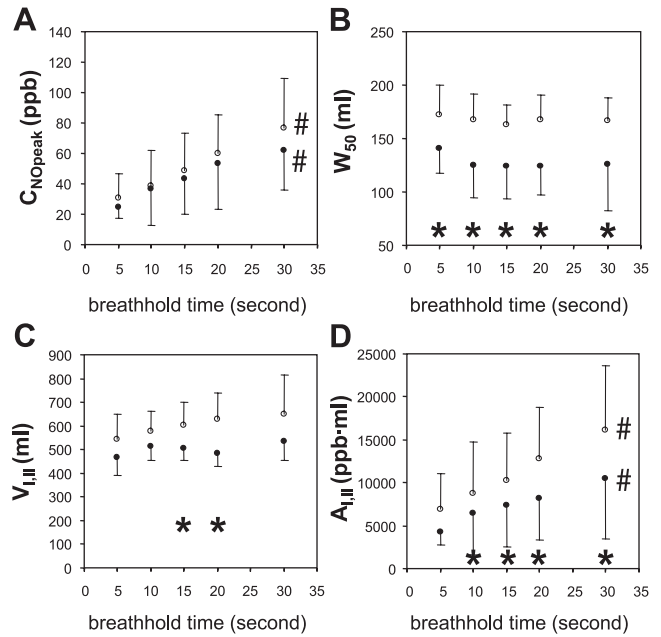


Fig. 3. Four parameters characteristic of phase I and II of the exhalation profile (Fig. 2A) that are model independent are presented for each of the different breath-hold times: $C_{NO\ peak}$ (A), W_{50} (B), $V_{I,II}$ (C) and $A_{I,II}$ (D). Open circles with lines represent the mean and standard deviation from air breathing, and solid circles with lines represent the mean and standard deviation from heliox breathing. #Statistically significant changes with breath-hold time (1-way ANOVA, $P < 0.05$). *Statistically significant difference between air and heliox breathing (paired t -test, $P < 0.05$).

DISCUSSION

This study characterized airway wall NO exchange dynamics using a newly developed breath-hold technique (21) that can more accurately determine the airway wall parameters (C_{awNO} , D_{awNO} , and J'_{awNO}), in particular D_{awNO} . The airway NO parameters should be independent of the physical properties of the insufflating gas (e.g., molecular diffusion coefficient) because they describe features of the airway wall or tissue. We utilized a trumpet model of the airway tree that considers axial diffusion of NO in the gas phase and demonstrated that a single set of airway wall parameters could simulate NO exchange dynamics with either air or heliox as the insufflating gas. We conclude that a trumpet model of the airway tree that considers axial diffusion captures the essential features of NO exchange in the airways. In addition, our results confirm earlier reports that loss of NO from the airways to the alveolar region by axial diffusion profoundly impacts airway wall NO characterization (21–23, 32) and that the airway wall concentration is more than an order of magnitude larger than previous estimates in healthy adults (21) utilizing models that neglected axial diffusion and the trumpet geometry of the airways.

Impact of Insufflating Gas

When heliox was used as the insufflating gas in the present study, exhaled NO concentration and thus the total mass of NO exhaled ($A_{I,II}$) was decreased (Figs. 2 and 3). The reduced $A_{I,II}$ is due primarily to the reduced W_{50} (thinner peak causes a small area) because $C_{NO\ peak}$ is independent of the insufflating gas (Fig. 2). Molecular diffusion of NO in helium is enhanced

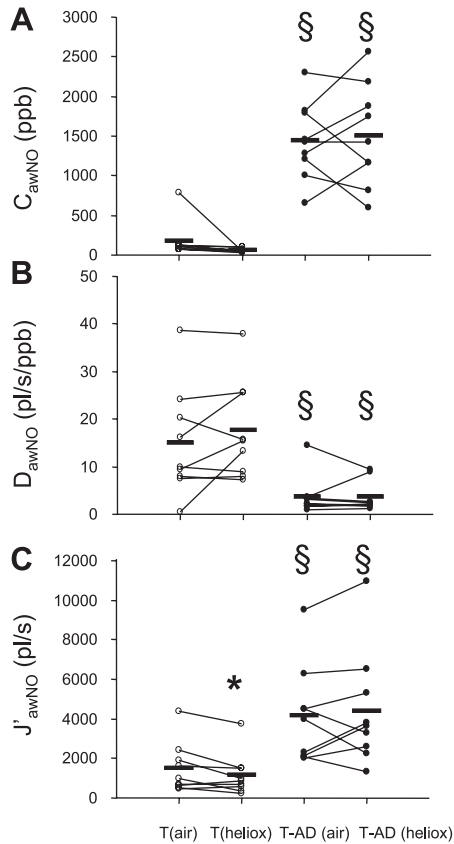


Fig. 4. Determined airway wall NO exchange parameters from trumpet-shaped airway: C_{awNO} (A), D_{awNO} (B), and J'_{awNO} (C) in the absence or presence of axial diffusion; T, trumpet model in the absence of axial diffusion; T-AD, trumpet model in the presence of axial diffusion. \circ , Each individual data point from model T; \bullet , each individual data point from model T-AD. Bars represent the mean. §Statistically significant difference among models (paired t -test, $P < 0.05$). *Statistically significant difference between air and heliox (paired t -test, $P < 0.05$).

relative to nitrogen. Thus, in the presence of heliox, the rate of molecular diffusion of NO is increased 2.3-fold. The reduced W_{50} represents depletion of NO in the smaller airways due to enhanced axial diffusion of NO from the airways to the alveolar region. $C_{NO\ peak}$ occurs in the first part of the exhaled breath, which is far away from the sink (i.e., the alveolar region) and is therefore not impacted by altering the rate of axial diffusion. This result is consistent with the concentration profile of NO in the airway tree as predicted by the trumpet model (Fig. 5) as well as previous reports (22, 23).

$V_{I,II}$ represents the volume of phase I and II of the exhaled profile as defined by the point of zero slope in the exhalation profile (Fig. 2A) and is therefore an estimate of that point in the exhalation when all airway gas has been expired by convection, including that in the respiratory transition region (i.e., generations 18-23). $V_{I,II}$ was statistically reduced in the presence of heliox for two of the five breath-hold times (Fig. 3C), and thus this trend may also explain the reduced $A_{I,II}$ observed for heliox. The trumpet model describes an abrupt transition between the airway and alveolar region, and this boundary is at a fixed concentration of $C_{ANO} = 0$. Thus the trumpet model structure, including the boundary conditions, dictates that a zero slope occurs at an exhaled volume equal to the volume of the trumpet (see Fig. 5) and that this volume would be inde-

pendent of the insufflating gas. However, it is also evident from Fig. 5 that the slope of the concentration profile becomes flatter at smaller volumes in the presence of heliox because of enhanced loss of NO to the alveolar region. This observation, combined with normal experimental noise and the fact that an abrupt transition between the airways and the alveolar region does not occur, may account for the experimental observations.

As shown in Fig. 4, airway wall NO parameters depend strongly on the insufflating gas when axial diffusion is neglected in the model (model T). In contrast, when axial diffusion is included (model T-AD), the airway wall NO parameters are independent of the insufflating gas. The airway wall NO parameters describe the airway wall tissue and depend on such characteristics as wall surface area, tissue thickness, and net rate of tissue production (28). Thus determined values for the airway wall NO parameters should be independent of the properties of the gas phase, such as the molecular diffusion coefficient. Indeed, we have previously demonstrated theoretically that the rate of radial diffusion of NO from the airway wall is independent of the gas phase (28). Our result suggests that a model of the airways that considers both trumpet geometry and axial diffusion captures the essential features of airway NO exchange.

Validity of the Model Assumptions and Structure

We assume that as z approaches zero, exhaled NO concentration in the gas phase of the airways (C_{NO}) approaches the steady-state alveolar concentration, C_{ANO} (Fig. 1). Although C_{ANO} has been shown by many investigators to be nonzero, the values are generally <2 ppb, much lower than those observed in the airway tree during the breath hold. Thus, for simplicity, C_{ANO} is set to zero as one of the boundary conditions. Van Muylem et al. (32) also explored the impact of axial diffusion of NO exchange by accounting for the trumpet shape of the airway tree. In their simulation, a zero C_{ANO} had minimal impact on the estimated steady-state NO concentration at 50 ml/s exhalation flow compared with $C_{ANO} = 1.8$ ppb (28.7 ppb vs. 29.8 ppb, respectively). Thus setting C_{ANO} to zero in the

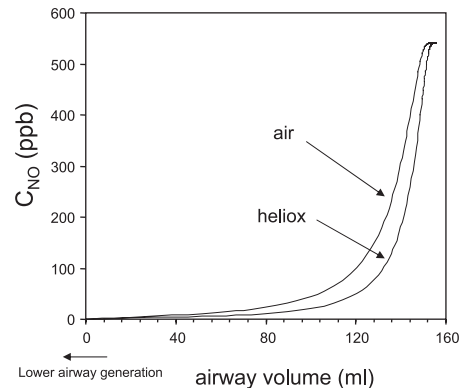


Fig. 5. C_{NO} as a function of volumetric position in the airway tree is shown for the T-AD model (see Fig. 1) for both air and heliox breathing when breath-hold time was set to 30 s. C_{awNO} was 1,439 ppb and D_{awNO} was $3.70 \text{ pl} \cdot \text{s}^{-1} \cdot \text{ppb}^{-1}$ for the simulation and represented the mean values of the 9 healthy subjects when breathing air. The presence of heliox (by changing the molecular diffusivity of NO from 0.23 to $0.52 \text{ cm}^2/\text{s}$) reduces the concentration of NO along the airway tree during breath hold but does not impact the maximum concentration of the NO within the airway.

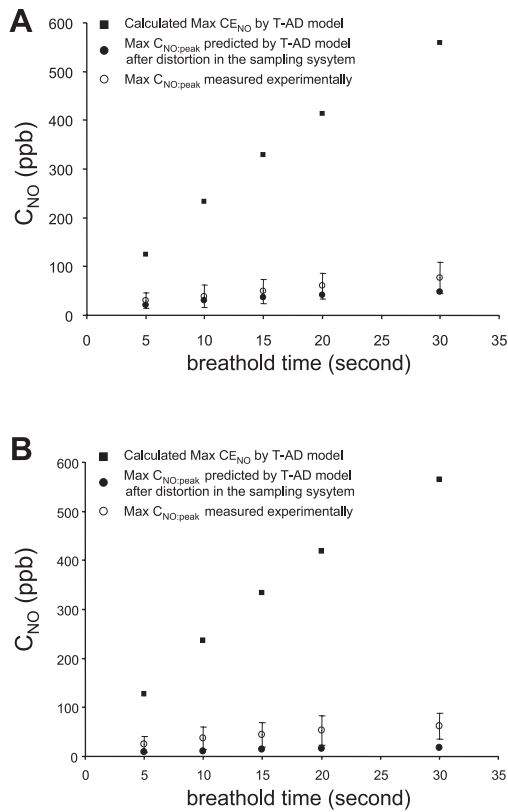


Fig. 6. Maximum NO concentrations in the exhaled profile for three cases at each breath-hold time. ■, Calculated maximum NO concentration exiting the mouth ($C_{E_{NO}}$; i.e., model prediction of peak NO concentration in expired gas) using mean values for best fit, airway wall parameters for air ($D_{aw_{NO}} = 3.70 \text{ pl}\cdot\text{s}^{-1}\cdot\text{ppb}$, $C_{aw_{NO}} = 1,439 \text{ ppb}$, A) and heliox ($D_{aw_{NO}} = 3.56 \text{ pl}\cdot\text{s}^{-1}\cdot\text{ppb}$, $C_{aw_{NO}} = 1,503 \text{ ppb}$, B); ●, model prediction of the maximum $C_{NO_{obs}}$ ($C_{NO_{peak}}$) in expired gas after distortion in the sampling system, on the basis of composite experimental NO tracing responses (see APPENDIX for details); ○, observed maximum NO concentration in expired gas ($C_{NO_{peak}}$). $C_{E_{NO}}$ enters the sampling system, which significantly flattens and broadens the exhaled profile because of dispersion introduced within the plumbing, leading to the analytical instrument, where the $C_{NO_{obs}}$ is actually measured. The result is a reduction in the peak height of $C_{NO_{obs}}$, compared with $C_{E_{NO}}$.

present simulation should have a minimal impact on the airway wall NO parameters.

The molecular diffusivity of NO ($0.52 \text{ cm}^2/\text{s}$ in heliox and $0.23 \text{ cm}^2/\text{s}$ in air) is an approximate value (19) and is assumed to be maintained in the airway trumpet (up to *generation 17*) during the breath hold. The molecular diffusivity of NO in the alveolar space is likely to be somewhere between these two values as the inspired heliox mixes with air in the residual volume (34). However, the fact that a pre-breath-hold tidal breathing wash-in period of heliox for 2 min has been shown not to impact exhaled NO concentrations (22) suggests that the rate-limiting location of axial diffusion for NO during the breath hold is not in the residual volume and alveolar space, but rather exists in small airways.

Accumulation of NO in the airway space during filling and evacuation of the airway tree before and after the breath hold may introduce error, which our model and parameter estimation algorithm do not consider. However, the subjects were instructed to inspire rapidly, generally over the course of $<3 \text{ s}$, and thus maintained an average inspiration flow of $>1 \text{ l/s}$. Thus filling of the airway tree at the end of inspiration would

generally take $<0.2 \text{ s}$ and could be considered negligible. The exhalation flow was recorded and was $>200 \text{ ml/s}$ [e.g., experimental average flow rate (SD) after the 20-s breath hold of air was 229 ml/s (SD 44)] to ensure evacuation of the airway space in $\sim 2 \text{ s}$. This delay may introduce an error, especially at the shorter breath-hold time (5 s). However, the 2-s delay would only be observed for the last part of the airway volume; thus the mean delay in the exhalation would be even smaller and is likely to be negligible.

Tissue Phase Concentration

Our estimated mean $C_{aw_{NO}}$ in healthy adults is $\sim 1,500 \text{ ppb}$ (1,439 and 1,503 ppb for air and heliox, respectively), which is more than an order of magnitude larger than that predicted by models that neglect axial diffusion and the shape of the airway tree, but consistent with our previous report using the breath-holding technique (21). This higher concentration approaches that capable of modulating smooth muscle tone. It has recently been demonstrated that soluble guanylate cyclase, the enzyme responsible for smooth muscle dilation, can be activated at NO concentrations as low as 3 ppm ($\sim 5 \text{ nM}$) (5). Thus, in asthma, in which exhaled NO concentrations can be increased by more than fivefold, airway wall concentrations may reach levels that impact airway and vascular smooth muscle tone.

During a breath hold, the concentration of NO in the airways increases because the concentration in the tissue phase (i.e., wall concentration, $C_{aw_{NO}}$) is larger than the gas phase. For a very long breath-hold time, the gas phase concentration, C_{NO} , would eventually reach $C_{aw_{NO}}$. Our estimated mean $C_{aw_{NO}}$ in healthy adults is much larger than the experimentally observed peak concentration of 77 and 62 ppb for air and heliox, respectively, after the largest breath-hold time of 30 s. This observation is consistent with our previous work (6, 21), and the discrepancy is due to two phenomena.

First, the sampling system introduces significant distortion of the observed exhaled profile due to axial dispersion (non-ideal flow) of the gas within the mouthpiece assembly and sampling line leading to the NO analyzer. This causes a pulse of NO to be significantly flattened (thus lowering the peak concentration) and broadened without altering the total mass of NO in the peak. This phenomenon was assessed theoretically in previous studies (6, 21), which accounted for axial dispersion within the sampling line. Herein, we have accounted for this effect experimentally (see APPENDIX). As presented in Fig. 6, $C_{NO_{obs}}(t)$ predicted by the T-AD model was calculated on the basis of experimental composite responses ($n = 20$) of NO tracings for both air and heliox as the carrier gas. These results are in good agreement with our experimental measurements for both air and heliox breathing. However, $C_{NO_{obs}}(t)$ predicted by model T-AD generates slightly lower values compared with experimentally observed $C_{NO_{peak}}$, which may be a consequence of averaging 20 experimental NO tracings to determine the composite responses. Other possible explanations are limitations on the precision of the tracer study (see APPENDIX) or that $C_{aw_{NO}}$ could be higher in the upper portion of the airway than in the lower airway (6).

The second reason why the observed gas concentration is less than $C_{aw_{NO}}$ is due to the observation that a steady state (or equilibrium) has not been reached with the gas phase. This can be observed by simply noting that $C_{NO_{peak}}$ after a 30-s breath-

hold time is significantly larger than that after the 20-s breath-hold time. The estimated mean time to reach 95% of equilibrium (i.e., C_{awNO}) is 128 s (2.13 min) for air and 218 s (3.63 min) for heliox breathing from the T-AD model. The longer time in the presence of heliox is a direct result of the enhanced loss of NO to the alveolar region, resulting in a smaller net (i.e., flux of the airway wall minus flux into the alveolar region) flux of NO into the gas phase.

In conclusion, utilizing a newly developed technique based on progressively increasing breath-hold times, this study investigated the impact of altering the properties of the insufflating gas on airway NO exchange. In the presence of heliox, the rate of NO diffusion is enhanced 2.3-fold and results in enhanced loss of airway NO to the alveolar region. A trumpet model that considers axial diffusion is able to accurately simulate this effect and predict airway NO exchange parameters in healthy adults that characterize airway wall tissue and are independent of the insufflating gas. A result of this model is the determination of airway wall concentrations in healthy adults that exceed 1 ppm, which is approximately an order of magnitude larger than estimates made with models that neglect the trumpet geometry and axial diffusion. This concentration approaches that capable of modulating airway smooth muscle tone and thus may be of clinical interest in disease states such as asthma that have elevated exhaled NO. We conclude that accurate estimation of flow-independent airway NO exchange parameters must include mathematical models that consider axial diffusion of NO in the gas phase and the trumpet shape of the airway tree.

APPENDIX

Distortion of NO Exhalation Profile by Sampling System

We performed a tracer study to investigate distortion of NO exhalation profiles by the sampling system (including the mouthpiece and sampling line). We injected 0.2 ml of 45 ppm NO (at a constant rate, over 1.56 s) into a diluent gas stream (~250 ml/s of either air or heliox). We then monitored the output response (solid lines, shown in Fig. A1, representing the averages of 20 NO tracings), which was significantly flattened and broadened for both air (mean $C_{NO\ peak}$ reduction of 48%, see Fig. A1A) and heliox (mean $C_{NO\ peak}$ reduction of 42%; see Fig. A1B). These results were sufficient to compute the impulse response (dashed lines shown in Fig. A1, scaled to yield NO masses equal to the pulse inputs for presentation), which relates the observed output response (measured data) to the expected input.

The present sampling system is identical to that described in a previous study (6). To mimic exhalation by a human subject, the injection was made at the entrance of the mouthpiece (located ~25 cm upstream of the sampling line inlet). From the injection point, the diluent gas first passes through an entrance region (~50 ml and 2.8-cm diameter) and then enters an in-line filter (~40 ml and 7-cm diameter) and traverses an exit region (~75 ml and 2.8-cm diameter) before it reaches the sampling point. We assumed that the injected NO was relatively well mixed within the entrance region, upstream of the filter. Thus we approximated the NO profile near the mouthpiece entrance as a 1.56-s duration stepwise, pulse ("square-wave") input (see gray shaded regions of Fig. A1). To check this assumption, we considered alternate orientations for administering the 45 ppm NO into the diluent gas stream and confirmed that these alternatives had little effect upon the measured response.

The scaled, impulse responses (shown in Fig. A1) were normalized to compute the "unit impulse responses" (transfer functions) for both air and heliox, on the basis of the tracer experiments. These transfer functions were then applied to the fitted T-AD model to predict the

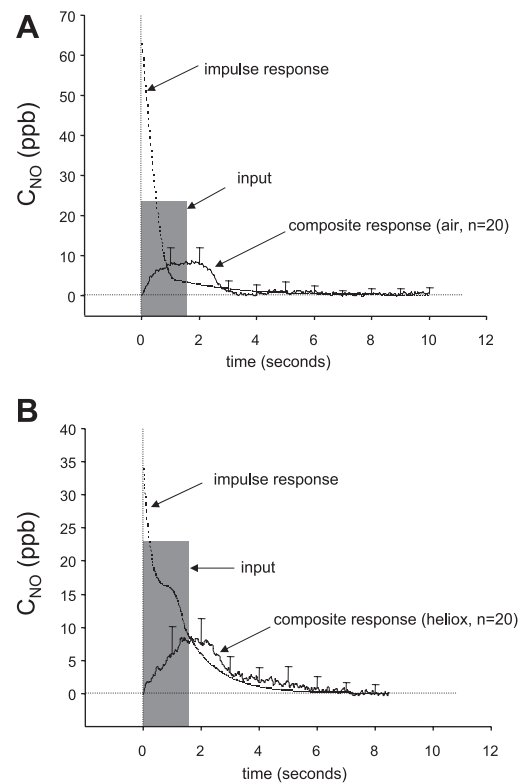


Fig. A1. Results of NO tracer analysis for air (A) and heliox (B). Experimental data for the composite response (solid lines, average, on the basis of 20 nitric oxide pulse tracings, with error bars representing standard deviation), estimated input (gray shaded regions), and calculated impulse response (dashed lines) were used to compute peak ratios from both air and heliox, composite, breath-hold tracings.

expected output response, on the basis of composite data for all nine subjects (see Fig. 6), which resulted in a potential $C_{NO\ peak}$ reduction of 6- to 30-fold.

These results should be interpreted prudently, because significant background noise limits resolution of the impulse response, which is based on composite averages of 20 tracer experiments and does not consider variation between these experiments. Furthermore, input NO profiles predicted by the fitted T-AD model are very sharp (0.1- to 0.2-s duration), compared with the tracer experiments (1.56-s duration), which leads to a much more significant reduction in $C_{NO\ peak}$. An alternative approach to the tracer results would be to deconvolve the NO concentration vs. time measurements from the breath-hold experiments directly, which would yield experimental estimates of $C_{NO\ peak}$ values (independent of any pulmonary model).

Finally, our assumption of a square-wave input (which may actually have been distorted at the mouthpiece entrance) for the tracer study could have resulted in overcorrection for $C_{NO\ peak}$ (the estimated exhaled peaks), on the basis of the fitted T-AD model. This would partially explain some of the discrepancies in Fig. 6, because $C_{NO\ peak}$ values predicted by the model (i.e., model predictions of peak NO in expired gas after distortion in the sampling system, denoted by solid circles in Fig. 6) are lower than the observed $C_{NO\ peak}$ values (i.e., observed peak NO in expired gas, denoted by open circles in Fig. 6).

ACKNOWLEDGMENTS

We thank the General Clinical Research Center at University of California, Irvine.

GRANTS

This work was supported by a grant from the National Heart, Lung, and Blood Institute (HL-070645).

REFERENCES

1. Alving K, Weitzberg E, and Lundberg JM. Increased amount of nitric oxide in exhaled air of asthmatics. *Eur Respir J* 6: 1368–1370, 1993.
2. ATS. Recommendations for standardized procedures for the online and offline measurement of exhaled lower respiratory nitric oxide and nasal nitric oxide in adults and children—1999. *Am J Respir Crit Care Med* 160: 2104–2117, 1999.
3. Barnes PJ and Kharitonov SA. Exhaled nitric oxide: a new lung function test. *Thorax* 51: 233–237, 1996.
4. Bui TD, Dabdub D, and George SC. Modeling bronchial circulation with application to soluble gas exchange: description and sensitivity analysis. *J Appl Physiol* 84: 2070–2088, 1998.
5. Condorelli P and George SC. In vivo control of soluble guanylate cyclase activation by nitric oxide: a kinetic analysis. *Biophys J* 80: 2110–2119, 2001.
6. Condorelli P, Shin HW, and George SC. Characterizing airway and alveolar nitric oxide exchange during tidal breathing using a three-compartment model. *J Appl Physiol* 96: 1832–1842, 2004.
7. George SC, Hogman M, Permutt S, and Silkoff PE. Modeling pulmonary nitric oxide exchange. *J Appl Physiol* 96: 831–839, 2004.
8. Girgis RE, Gugnani MK, Abrams J, and Mayes MD. Partitioning of alveolar and conducting airway nitric oxide in scleroderma lung disease. *Am J Respir Crit Care Med* 165: 1587–1591, 2002.
9. Gustafsson LE, Leone AM, Persson MG, Wiklund NP, and Moncada S. Endogenous nitric oxide is present in the exhaled air of rabbits, guinea pigs and humans. *Biochem Biophys Res Commun* 181: 852–857, 1991.
10. Hogman M, Drca N, Ehrstedt C, and Merilainen P. Exhaled nitric oxide partitioned into alveolar, lower airways and nasal contributions. *Respir Med* 94: 985–991, 2000.
11. Hogman M, Holmkvist T, Wegener T, Emtner M, Andersson M, Hedenstrom H, and Merilainen P. Extended NO analysis applied to patients with COPD, allergic asthma and allergic rhinitis. *Respir Med* 96: 24–30, 2002.
12. Lehtimäki L, Kankaanranta H, Saarelainen S, Hahtola P, Jarvenpää R, Koivula T, Turjanmaa V, and Moilanen E. Extended exhaled NO measurement differentiates between alveolar and bronchial inflammation. *Am J Respir Crit Care Med* 163: 1557–1561, 2001.
13. Lehtimäki L, Turjanmaa V, Kankaanranta H, Saarelainen S, Hahtola P, and Moilanen E. Increased bronchial nitric oxide production in patients with asthma measured with a novel method of different exhalation flow rates. *Ann Med* 32: 417–423, 2000.
14. Mahut B, Delclaux C, Tillie-Leblond I, Gosset P, Delacourt C, Zerh-Lancner F, Harf A, and de Blic J. Both inflammation and remodeling influence nitric oxide output in children with refractory asthma. *J Allergy Clin Immunol* 113: 252–256, 2004.
15. Paiva M and Engel LA. Pulmonary interdependence of gas transport. *J Appl Physiol* 47: 296–305, 1979.
16. Payne DN, Adcock IM, Wilson NM, Oates T, Scallan M, and Bush A. Relationship between exhaled nitric oxide and mucosal eosinophilic inflammation in children with difficult asthma, after treatment with oral prednisolone. *Am J Respir Crit Care Med* 164: 1376–1381, 2001.
17. Pedroletti C, Hogman M, Merilainen P, Nordvall LS, Hedlin G, and Alving K. Nitric oxide airway diffusing capacity and mucosal concentration in asthmatic schoolchildren. *Pediatr Res* 54: 496–501, 2003.
18. Pietropaoli AP, Perillo IB, Torres A, Perkins PT, Frasier LM, Utell MJ, Frampton MW, and Hyde RW. Simultaneous measurement of nitric oxide production by conducting and alveolar airways of humans. *J Appl Physiol* 87: 1532–1542, 1999.
19. Reid RC, Frausnitz JM, and Poling BE. *The Properties of Gases and Liquids*. New York: McGraw-Hill, 1988.
20. Scherer PW, Gobran S, Aukburg SJ, Baumgardner JE, Bartkowski R, and Neufeld GR. Numerical and experimental study of steady-state CO₂ and inert gas washout. *J Appl Physiol* 64: 1022–1029, 1988.
21. Shin HW, Condorelli P, and George SC. A new and more accurate technique to characterize airway nitric oxide using different breathhold times. *J Appl Physiol* 98: 1869–1877, 2005.
22. Shin HW, Condorelli P, Rose-Gottron CM, Cooper DM, and George SC. Probing the impact of axial diffusion on nitric oxide exchange dynamics with heliox. *J Appl Physiol* 97: 874–882, 2004.
23. Shin HW and George SC. Impact of axial diffusion on nitric oxide exchange in the lungs. *J Appl Physiol* 93: 2070–2080, 2002.
24. Shin HW, Rose-Gottron CM, Cooper DM, Newcomb RL, and George SC. Airway diffusing capacity of nitric oxide and steroid therapy in asthma. *J Appl Physiol* 96: 65–75, 2004.
25. Shin HW, Rose-Gottron CM, Perez F, Cooper DM, Wilson AF, and George SC. Flow-independent nitric oxide exchange parameters in healthy adults. *J Appl Physiol* 91: 2173–2181, 2001.
26. Shin HW, Rose-Gottron CM, Sufi RS, Perez F, Cooper DM, Wilson AF, and George SC. Flow-independent nitric oxide exchange parameters in cystic fibrosis. *Am J Respir Crit Care Med* 165: 349–357, 2002.
27. Silkoff PE, Sylvester JT, Zamel N, and Permutt S. Airway nitric oxide diffusion in asthma: role in pulmonary function and bronchial responsiveness. *Am J Respir Crit Care Med* 161: 1218–1228, 2000.
28. Tsoukias NM and George SC. A two-compartment model of pulmonary nitric oxide exchange dynamics. *J Appl Physiol* 85: 653–666, 1998.
29. Tsoukias NM, Shin HW, Wilson AF, and George SC. A single-breath technique with variable flow rate to characterize nitric oxide exchange dynamics in the lungs. *J Appl Physiol* 91: 477–487, 2001.
30. Tsoukias NM, Tannous Z, Wilson AF, and George SC. Single-exhalation profiles of NO and CO₂ in humans: effect of dynamically changing flow rate. *J Appl Physiol* 85: 642–652, 1998.
31. Tsujino I, Nishimura M, Kamachi A, Makita H, Munakata M, Miyamoto K, and Kawakami Y. Exhaled nitric oxide—is it really a good marker of airway inflammation in bronchial asthma? *Respiration* 67: 645–651, 2000.
32. Van Muylem A, Noel C, and Paiva M. Modeling of impact of gas molecular diffusion on nitric oxide expired profile. *J Appl Physiol* 94: 119–127, 2003.
33. Weibel ER. *Morphometry of the Human Lung*. Berlin: Springer-Verlag, 1963.
34. Worth H, Nusse W, and Piiper J. Determination of binary diffusion coefficients of various gas species used in respiratory physiology. *Respir Physiol* 32: 15–26, 1978.